CrossMark

ORIGINAL PAPER

Hierarchical porous cellulose/activated carbon composite monolith for efficient adsorption of dyes

Qiuhong Bai · Qiancheng Xiong · Cong Li · Yehua Shen · Hiroshi Uyama

Abstract Cheap and efficient adsorbents to remove contaminants of toxic dye molecules from wastewater are strongly in demand for environmental reasons. This study provides a novel design of a monolithic adsorbent from abundant materials via a facile synthetic procedure, which can greatly reduce the problems of the tedious separation of adsorbents from treated wastes. A hierarchically porous cellulose/ activated carbon (cellulose/AC) composite monolith was prepared by thermally-induced phase separation of cellulose acetate in the presence of AC, using a mixture of DMF and 1-hexanol, followed by alkaline hydrolysis. The composite monolith had a large specific surface area with mesopore distribution. It not only showed high uptake capacity towards methylene blue (MB) or rhodamine B (RhB) but could also simultaneously adsorb MB and RhB from their mixture, in which the adsorption of one dye was not influenced by the other one. Remarkable effects of solution pH, initial concentration of dye (C_0), contact time, adsorbent dosage and temperature on the adsorption of MB and RhB onto the composite monolith were demonstrated. The binding data for MB and RhB adsorption on the composite monolith fitted the Freundlich model well, suggesting a heterogeneous surface of the composite monolith. The monolith could retain around 90% of its adsorption capacity after 8 times reuse. These data demonstrate that the cellulose/AC composite monolith has a large potential as a promising adsorbent of low cost and convenient separation for dye in wastewater.

Q. Bai · Q. Xiong · C. Li · Y. Shen (✉) ·
H. Uyama (✉)
Key Laboratory of Synthetic and Natural Functional
Molecule Chemistry of Ministry of Education, College of
Chemistry and Materials Science, Northwest University,
Xi'an 710127, China
e-mail: yhshen@nwu.edu.cn

H. Uyama
e-mail: uyama@chem.eng.osaka-u.ac.jp

H. Uyama
Department of Applied Chemistry, Graduate School of
Engineering, Osaka University, Suita 565-0871, Japan

Introduction

Discharged dyes in wastewater pose significant threats to the aqueous environment and human health, and also have an economic impact. Therefore, the removal of toxic dyes in wastewater is an extremely urgent issue. Adsorption is considered a simple, low-cost and eco-friendly technology to remove such dyes (Dong et al. 2014; Yi et al. 2015).

Cellulose is the most abundant natural polymer with high hydrophilicity due to its natural structure. Cellulose shows good mechanical strength and solvent tolerance toward water and common organic solvents. Owing to their characteristic features, cellulose and its composites have been applied in the fields of energy, catalysis, medical science, environmental engineering, separation and filtration (Gopiraman et al. 2015). Cellulose and its modified derivatives have been used for adsorption of toxic heavy metals such as Pb^{2+} (Wu et al. 2012) and dyes (Dridi-Dhaouadi et al. 2011). However, their capacity for adsorption of these toxic compounds is often limited. To solve this issue, a composite of magnetic cellulose, Fe_3O_4 and activated carbon was developed for the removal of congo red (Zhu et al. 2011). An ethylenediamine-modified nanofibrillated cellulose/chitosan composite was used for the adsorption of cationic and anionic dyes (Liu et al. 2016).

Monoliths, single pieces with a three-dimensional (3D) hierarchical porous architecture, fast mass transfer property, good permeability, and high stability, have been widely utilized for separation and adsorption. Recently, the fabrication of polymer-based monoliths by thermally-induced phase separation (TIPS) of polymer solutions has received enormous interest for various applications. So far, polymer monoliths have been obtained by TIPS from a variety of polymers such as polyacrylonitrile (PAN), polycarbonate, poly(vinyl alcohol) (PVA), poly(ethylene-*co*-vinyl alcohol) (EVOH), poly(γ-glutamic acid) and poly(methyl methacrylate) (Okada et al. 2011; Xin et al. 2012; Sun et al. 2013; Wang and Uyama 2015; Park et al. 2013; Yoneda et al. 2014). By using TIPS, the shapes of monoliths can be tuned by altering the vessel shape. More importantly, the porous structure can be readily controlled by changing the phase separation conditions. This method has also been expanded to blend monoliths such as EVOH/chitosan, PVA/sodium alginate, and polycarbonate/poly(3-hydroxyalkanoate) (Wang et al. 2015; Sun and Uyama 2013).

Porous carbon materials, a typical example being AC with a high surface area (700–1500 m^2 g^{-1}) (He et al. 2013), are used industrially as adsorbents for various organic and inorganic compounds (Lillo-Ródenas et al. 2010; Choong et al. 2006). Most carbon materials possess microporous structures having low efficiency towards the removal of compounds with high molecular weight (Balathanigaimani et al.

2008, 2009; Menon and Komarneni 1998). Moreover, powders of activated carbon (AC) cannot be easily handled and separated from an aqueous solution, making subsequent operations difficult and/or tedious. Thus, novel adsorbents with mesoporous structure (2–50 nm) in a suitable shape for easy operation are greatly required in industrial applications. Monoliths may be good candidates for the removal of toxic compounds in environmental engineering by utilizing their characteristic features such as fast mass transfer property and good permeability.

In the TIPS process for the fabrication of polymeric monoliths, the polymer is first dissolved in a suitable mixture of solvent by heating. If functional inorganic compounds with good adsorption ability such as AC and zeolite can be well dispersed in this polymer solution, and the dispersity is kept during the phase separation in the cooling step, a composite monolith consisting of the polymer and an inorganic compound will be obtained. Polymeric monoliths often possess a small specific surface area, which limits practical applications as adsorbents; on the other hand, composite monoliths with mesoporous inorganics including AC can afford a large surface area, which is suitable for the adsorption of toxic compounds. On the basis of the above design, we have prepared a cellulose/AC composite monolith and examined the dye adsorption.

Very recently, we fabricated a porous cellulose monolith by TIPS. Due to the very low solubility of cellulose in water and common organic solvents, cellulose acetate (CA) was selected as starting polymer for fabrication of cellulose monolith. The phase separation of the CA solution by TIPS produced a CA monolith, which was easily converted to a cellulose monolith by selective alkaline hydrolysis of the side chain in the CA (Xin et al. 2017).

The present research aims at the development of a functionally porous composite monolith of cellulose and AC with a morphology precisely controlled by TIPS and the evaluation of its practical utilization for water treatment. A cationic dye, methylene blue (MB), and a betaine dye, rhodamine B (RhB), were selected as model dyes for removal by the composite monolith. Two systems, a single-dye aqueous solution and the MB/RhB mixed aqueous solution, were used for the adsorption evaluation. The present monolith with hierarchically porous structure showed good adsorption ability for both MB and RhB. The adsorption

isotherms and kinetic parameters were evaluated in detail. The present study provides a facile fabrication method of composite monoliths of polymers and functional inorganics for various applications including wastewater treatment. Many combinations of polymers and functional inorganics can be available to introduce the inorganics into polymer monoliths, which further expands applications of polymer monoliths prepared by TIPS (Radha et al. 2017).

Experimental section

Materials

CA with molecular weight of 5×10^4 (39.3–40.3 wt% of acetyl content) was purchased from Sigma-Aldrich. Activated carbon for water purification and gas adsorption was bought from Aladdin Industrial. MB ($\lambda = 664$ nm) was kindly offered by the Tianxin Fine Chemicals Development Center. 1-Hexanol was obtained from the TianJin Guangfu Fine Chemical Research Institute. RhB ($\lambda = 553$ nm), dimethyl sulfoxide (DMSO), N, N-dimethylformamide (DMF), KH_2PO_4, Na_2HPO_4, ethanol and sodium hydroxide (NaOH) were obtained from TianJin Zhiyuan Chemical Industries. All chemicals and reagents were of analytical grade and used without further purification.

Measurements

FTIR spectra of monoliths were obtained using a TENSOR27 (Bruker, Germany) Fourier transform infrared spectrometer to examine the surface functional groups of monoliths. Structure and morphology of monoliths were observed with scanning electron microscopy (SEM) (SU3500; Hitachi, Tokyo, Japan) at 15 kV. The samples must be coated with a thin layer of gold (E-1010 Ion Sputter; Hitachi) before the SEM images are obtained. The pore structure of the samples was analyzed by N_2 adsorption/desorption isotherms with a TR2 Star3020 Surface Area and Pore Size Analyzer at 77 K. The Brunauer–Emmett–Teller (BET) method was used to measure the specific surface area. Thermogravimetric analysis (TGA) was conducted with NETZSCH STA 449C with a heating rate of 10 °C min^{-1} under high-purity nitrogen (from 33 to 900 °C). Absorbance measurements of dyes in aqueous solutions were made with a UV-1700 (SHIMADZU, Japan) UV–vis spectrometer.

Fabrication of CA/AC composite monolith

The preparation of the composite monolith was performed according to the typical fabrication method of the CA monolith using DMF as solvent and 1-hexanol as non-solvent (Fig. 1). CA powder (4.0 g) was dissolved in 20 mL of DMF under gentle stirring at 70 °C. Then, 20 mL of 1-hexanol was added dropwise into the CA solution in two parts to prevent the generation of precipitates. AC (2.0 g) powder was dispersed in the CA solution. Finally, 10 mL of 1-hexanol was added and the mixture was gently stirred at 70 °C. After 1 day, it was cooled to 20 °C and kept overnight, during which phase separation took place. The as-obtained gel was immersed into a large amount of ethanol three times to remove the solvents, and subsequently dried under vacuum at ambient temperature for 12 h to give the CA/AC composite monolith.

Fabrication of cellulose/AC composite monolith

The cellulose/AC monolith was obtained by hydrolysis of the CA/AC monolith under alkaline condition. The CA/AC monolith (2 g) was soaked in 80 mL of methanol for 3 h under gentle stirring. Then, 6 mL of 2 M NaOH methanol solution was poured into the solution and the hydrolysis was carried out at room temperature for 3 h. The solution was neutralized with 1 M HCl and the monolith was washed with a large amount of water. Finally, the medium in the monolith was successively replaced with methanol and the monolith was dried under vacuum at room temperature.

Preparation stock solutions of dyes

A typical configuration process of MB stock solution was based on GB/T 12496.10-1999. At first, a phosphate buffer solution of pH 7 was prepared by dissolving Na_2HPO_4 (14.3 g) and KH_2PO_4 (3.6 g) in 1000 mL of deionized water. A stock solution of MB with the concentration of 1000 mg L^{-1} was prepared by dissolving MB (1.0 g) in the phosphate buffer solution. A stock of RhB with the same concentration was made by dissolving 1.0 g of RhB into 1000 mL of

Fig. 1 A general procedure for fabrication of a cellulose/AC composite monolith

deionized water. The dye solution with the desired concentration was obtained by diluting the stock solution.

Adsorption experiments

The adsorption experiments were divided into (1) adsorption of a single dye and (2) simultaneous adsorption of two dyes. The adsorption of dyes from aqueous solutions by the composite monolith was performed by a batch system to evaluate the adsorption capacities and adsorption kinetics. Generally, adsorption is influenced by various experimental parameters (Kyzas and Bikiaris 2015). In this study, the effects of initial pH, initial dye concentration, contact time, adsorbent dosage and temperature on the removal of RhB and MB were systematically examined. The adsorption procedure of MB and RhB on the monolith is as follows.

Adsorption of a single dye (MB or RhB)

The dye adsorption capacity of the cellulose monolith and the cellulose/AC composite monolith was compared. The monolithic adsorbent (0.1 g) was placed into a 250-mL conical flask containing 25 mL of 200 mg L^{-1} dyes solution (RhB or MB). The adsorption experiments were carried out by continuously agitating the dye solution including the monolith at 150 rpm in a thermostatic shaker at 298 K. The monolithic adsorbent was separated from the solution and the dye concentration was measured by UV–vis spectroscopy at the maximum wavelength of the dye (MB: 663 nm; RhB: 553 nm). The adsorption at

different times was examined until the adsorption reached the equilibrium, and the experiments were performed at least three times. The adsorption capacity at contact time t was calculated as follows:

$$q_t = (C_0 - C_t) \times V/m$$

where q_t (mg g^{-1}) and C_t (mg L^{-1}) represent the adsorption capacity and dye concentration at contact time t, respectively. C_0, V and m (g) are the initial concentration of the dye, the volume of the dye solution, and the mass of absorbent, respectively.

The effect of pH on the adsorption was studied in the pH range of 1–11, and the pH of solution was adjusted by adding 0.1 M HCl or 0.1 M NaOH. The adsorption capacity at the equilibrium was measured. The equilibrium capacity, q_e (mg g^{-1}), was calculated as follows:

$$q_e = (C_0 - C_e) \times V/m$$

where C_e (mg L^{-1}) is the dye concentration at the equilibrium.

To study the effect of contact time and initial concentration of the dyes, batch experiments were carried out under the following conditions to determine the equilibrium capacity: initial concentrations of 10, 50, 100, 200, 300, 400, 500 mg L^{-1}; pH 7 (MB), pH (RhB); temperature: 298 K; and adsorbent dosage of 0.10 g per 25 mL of a dye solution.

Different amounts of the cellulose/AC composite monolith (0.05–0.40 g) were used to examine the percentage of the dye adsorption. The adsorption experiment was performed under the following conditions: initial concentration of 200 mg L^{-1}; pH 7 (MB), pH 3 (RhB); and temperature: 298 K. The

removal efficiency of dye was calculated by the following equation:

$$\text{Removal efficiency } (\%) = [(C_0 - C_t)/C_0] \times 100$$

where C_0 (mg L^{-1}) and C_t (mg L^{-1}) are the concentrations of dye before and after the adsorption, respectively.

The effect of temperature was examined at 298, 313 and 333 K. The experiment was conducted under the following conditions: initial concentration of 200 mg L^{-1}; pH 7 (MB), pH 3 (RhB); and adsorbent dosage: 0.1 g per 25 mL. The experimental temperature was adjusted by a water bath thermostat.

Simultaneous adsorption of MB and RhB mixture

All the experimental processes and conditions were the same for the aforementioned operations except the use of the mixed solution of MB and RhB with a concentration of 200 mg L^{-1}. Both dyes were adsorbed simultaneously at pH 7, and the concentrations were detected in a constant contact time.

Kinetics and isotherms

The kinetic data were analyzed by pseudo-first-order (Lagergren 1898) and pseudo-second-order (Ho and McKay 1999) rate equations, which can be expressed as:

The pseudo-first-order: $\quad \ln(q_e - q_t) = \ln q_e - k_1 t$

The pseudo-second-order: $\quad t/q_t = 1/(k_2 q_e^2) + t/q_e$

where k_1 (min^{-1}) and k_2 [g (mg min)$^{-1}$] are the pseudo-first-order and pseudo-second-order rate constants, respectively. The plots of $\ln(q_e - q_t)$ against t are expected as a linear graph with a slope $-k_1$ and intercept of $\ln q_e$, and q_e was calculated according to the intercept of the fitted linear, called the calculated value of adsorption capacity ($q_{e, cal}$). For the pseudo-second-order, a linear graph is obtained from a plot of t/q_t against t with a slope $1/q_e$ and intercept $1/(k_2 q_e^2)$, and q_e was calculated according to the slope of the fitted linear, called the calculated value of adsorption capacity ($q_{e, cal}$).

The Freundlich and Langmuir models (Freundlich 1906; Langmuir 1916) are the most universal equations to fit experimental data in equilibrium. The Langmuir isotherm assumes that an adsorbent surface has homogeneous binding sites, monolayer coverage, and no interactions between adsorbed species. The Freundlich isotherm is based on multilayer of heterogeneous surfaces; both models are expressed as follows:

Langmuir model: $\quad C_e/q_e = C_e/q_{max} + 1/(q_{max}K_L)$
Freundlich model: $\quad \ln q_e = 1/n \ln C_e + \ln K_F$
Langmuir model: $\quad q_{max} = q_e(1 + C_e K_L)/C_e K_L$

where q_{max} (mg g^{-1}) is the Langmuir constant related to maximum adsorption capacity, and K_L (L mg^{-1}) represents the Langmuir constant related to binding affinity. In the case of the Langmuir model, the plot of C_e/q_e gives a straight line with a slope and intercept of $1/q_{max}$ and $1/q_{max}K_L$, respectively. For the Freundlich model, K_F [(mg g^{-1}) (L mg^{-1})$^{1/n}$] and n are the characteristic Freundlich constants, which show the adsorption capacity and the adsorption intensity, respectively. The plot of $\ln q_e$ against $\ln C_e$ gives a linear relationship with slope of $1/n$ and intercept $\ln K_F$.

Desorption and recyclability

To test the desorption of MB and RhB, the composite monolith (0.10 g) was added to 25 mL of MB (400 mg mL^{-1}) or RhB (400 mg mL^{-1}) solution and kept for 60 h under gentle shaking at 150 rpm, and the residual concentration was measured by UV–vis spectroscopy. The composite monolith was then immersed in 99% of ethanol solution for desorption of the MB or RhB molecules. The recyclability was tested by repeating the same experiments 8 times.

Results and discussion

Fabrication and morphology characterization of cellulose/AC monolith

For the preparation of monoliths from polymer solutions by the TIPS method, the selection of solvent composition and polymer concentration are crucial factors to control (TIPSthree-dimensional continuous porous structure of the monoliths. It is very difficult for cellulose to dissolve in common solvents. However, its derivatives, typically CA, could be dissolved in organic solvents such as DMF and DMSO. Very

recently, we have achieved the fabrication of a CA monolith by the TIPS method using DMF as the solvent and 1-hexanol as the non-solvent, and systematically examined the fabrication parameters to tune the porous structure of the monolith (Xin et al. 2017). In this study, the CA monolith was prepared from a combination of DMF and 1-hexanol as well as of DMSO and water.

In case of the DMF/1-hexanol mixture (40:60 vol%), CA was first dissolved in DMF with the CA concentration of 200 mg mL^{-1} at heating, and then 1-hexanol was added dropwise to avoid the formation of precipitates (final CA concentration: 80 mg mL^{-1}). In the cooling step, the liquid/solid phase separation occurred quickly to form the monolith. For the combination of DMSO and water (75/25 vol%), CA could be dissolved in the mixture with the CA concentration of 100 mg mL^{-1} at heating, and the obtained solution was subjected to the phase separation by cooling, producing the CA monolith. SEM images of the CA monolith using the different phase separation solvents are shown in Fig. 2 (DMF + 1-hexanol) and S1. For the mixed solvent of DMF and 1-hexanol, a three-dimensional (3D) open pore structure with a columnar skeleton was observed

(Figs. 2a, S1a), whereas a branch-connected morphology was found for the mixed solvent of DMSO and water (Fig. S1c), and the skeleton size was somewhat smaller than that of the DMF/1-hexanol mixture. The reason may be due to the different separation between the polymer-rich phase and the polymer-lean phase for the two systems and the different polymer concentration suitable for monolith formation, resulting in the growth of the monolith skeleton with different morphology and structure. Another obvious difference of the two solvent systems was the shape of the obtained monolith, as the shape from the DMF/1-hexanol mixture was much better than that from the DMSO/water. Additionally, the fabrication process was more facile for the former. Thus, a mixture of DMF and 1-hexanol was mainly used as the phase separation solvent in this study.

Next, the fabrication of an AC-containing composite monolith was examined. Various AC powders are commercially available. AC powders suitable for the good dispersion in the phase separation solvent were screened, and AC of 200 mesh was found to be dispersed uniformly in the CA solution under the intense stirring. The general fabrication process of a cellulose/AC composite monolith is shown in Fig. 1.
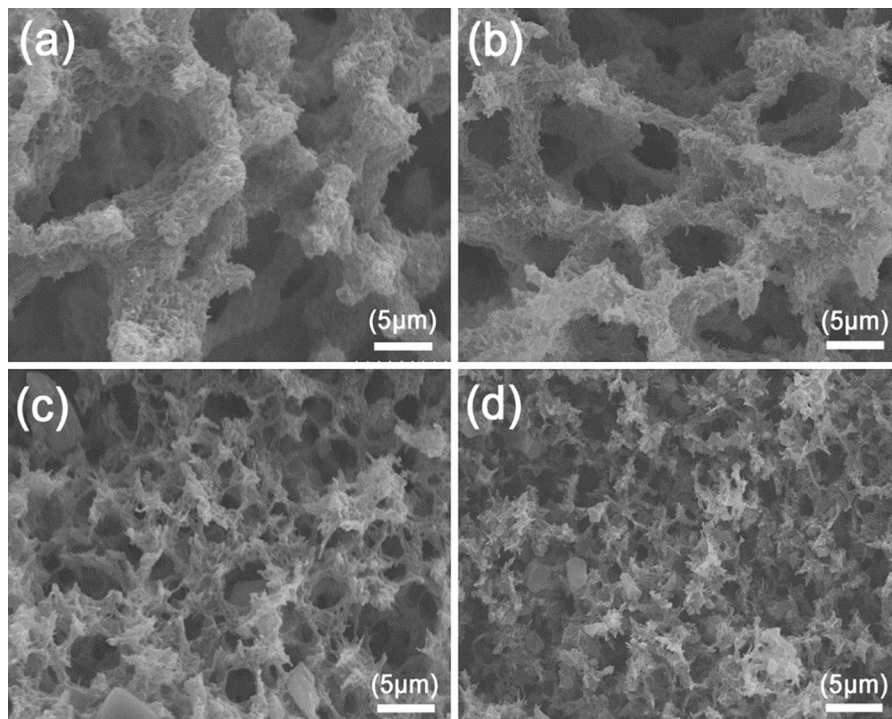
Fig. 2 SEM images of CA monolith (**a**), cellulose monolith (**b**), CA/AC monolith (**c**), and cellulose/AC composite monolith (**d**)

The fabrication conditions are as follows: DMF/1-hexanol mixed ratio of 2/3, CA concentration of 80 mg mL^{-1}, AC amount of 40 mg mL^{-1}, and cooling temperature of 20 °C. SEM images of the CA/AC composite monolith show that AC with the irregular sheet-like structure was loaded in the pore structure of the monolith (Fig. 2c), suggesting that the composite material was prepared successfully. By the addition of AC, the skeleton size of the CA monolith greatly decreased, suggesting that AC strongly affected the phase separation process of the CA solution.

Previously, we found that the selective alkaline hydrolysis of the acetyl group of CA in the monolith proceeded in methanol (Xin et al. 2017). The morphology of the present CA monolith prepared from DMF/1-hexanol or DMSO/water was not changed by the alkaline hydrolysis (Figs. 2, S1). Thus, a cellulose/AC composite monolith was fabricated by hydrolysis of the CA/AC monolith in NaOH methanol solution. Intriguingly, the monolithic shape and porous morphology of the resultant cellulose/AC monolith still remained after the hydrolysis (Fig. 2d), demonstrating that the current hydrolysis conditions were preferable for the fabrication of the cellulose/AC monolith, whereas the skeleton surface of the cellulose/AC monolith became slightly rough in comparison with that of the CA/AC monolith, and its skeleton size slightly decreased, indicating the generation of smaller pores for the cellulose/AC monolith, resulting in the large surface area, as discussed later. The mesoporous structure inside the cellulose/AC monolith offered sufficient space for the passage of dye molecules.

The hydrolysis of the acetyl group in the CA/AC monolith was confirmed by FT-IR (Fig. S2). After the hydrolysis, the strong adsorption band at 1730 cm^{-1}, the characteristic of the stretching vibration of C=O, completely disappeared. Moreover, the peak intensity around 3400 cm^{-1} corresponding to the O–H stretching vibration, increased after the hydrolysis. These results indicate that the acetyl group in the CA/AC composite monolith was completely hydrolyzed under the present conditions, and that methanol is the recommended choice as a solvent to selectively hydrolyze the side chain in CA.

N$_2$ adsorption/desorption isotherm

Nitrogen adsorption/desorption isotherms of the two types of monoliths are shown in Fig. 3a. The cellulose monolith presented a typical IV curve, while the composite monolith exhibited a type I/IV isotherm, indicating the formation of a mesoporous material. A pronounced hysteresis loop of type H1 was observed in the P/P_0 ranging from 0.45 to 1 for the composite monolith, while the hysteresis of the cellulose monolith starting at $P/P_0 \approx 0.8$ demonstrated sharp capillary condensation. The hysteresis of the cellulose/AC monolith suggested cylindrical pores or slit-type pores, corresponding to its irregular structure with narrow pore size distribution (Coleman and Hench 2000; He et al. 2013). Furthermore, a slight increase of nitrogen adsorbing quantity for composite monolith was observed at low relative pressure, indicating the formation of a few micropores. More importantly, the obviously steep tails at $p/p_0 = 0.9$ demonstrated the existence of macropores in both samples. The horizontal branch near the saturation pressure (p/p_0 range from 0.2 to 0.9) indicated that almost all the mesopores could be filled with dye molecules. A remarkable difference of pore size distribution for two types of the monoliths is exhibited in Fig. 3b. A sharp peak around 4.9 nm was observed in the composite monolith. This reveals that mesopores are dominant for the cellulose/AC composite, and that the pore channel is beneficial for the adsorption of macromolecules. On the other hand, the cellulose monolith possessed a broad pore range including mesopores and macropores. Therefore, it can be concluded that the cellulose/AC monolith with a hierarchical porous structure was successfully prepared.

Table 1 summarizes the specific surface areas, pore volumes and mean pore diameters of the cellulose monolith and the cellulose/AC composite monolith. The specific surface area and pore volume of the cellulose/AC composite monolith were much larger than those of the cellulose monolith, which can be explained by the addition of AC enlarging the specific surface area and pore volume of the composite monolith. The mean pore diameter was in close agreement with the pore size distribution for both monoliths.

Thermogravimetric analysis

TGA was used to investigate the thermostability of the cellulose monolith and cellulose/AC composite monolith (Fig. S3). For the cellulose monolith, two main steps of decomposition were observed. The small

Fig. 3 Nitrogen
adsorption–desorption
isotherms (**a**), pore size
distribution curve (**b**) of
cellulose monolith and
cellulose/AC composite
monolith by NLDFT
method
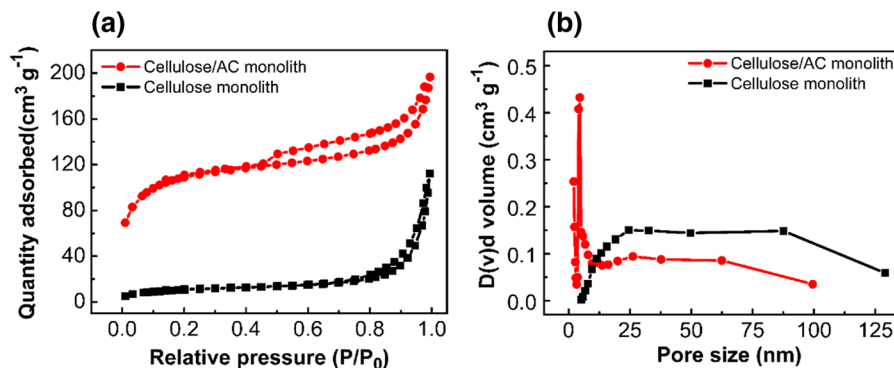
Table 1 Specific surface areas, pore volumes and mean pore diameters of the cellulose and cellulose/AC composite monoliths

Sample	Specific surface area (m^2 g^{-1})	Pore volume (cm^3 g^{-1})	Mean pore diameter (nm)
Cellulose monolith	36.8	0.104	11.3
Cellulose/AC	348	0.261	3.00

weight change was firstly observed in the temperature range from 120 to 230 °C, in which the depolymerization of cellulose occurred slowly. This degradation is called the "vitrification" phenomenon (Bradbury et al. 1979). The second step was the decomposition of cellulose from 300 to 400 °C, in which a rapid weight decrease was found. The cellulose/AC composite monolith also showed apparent thermal decomposition in the temperature range from 280 to 400 °C. Initial slight decomposition from 33 to 100 °C of both monoliths might be mainly due to the loss of water contained in the monolith. The weight loss values of the cellulose monolith and cellulose/AC monolith at 900 °C were 88 and 62%, respectively. The weight ratio of cellulose and AC in the composite monolith could be calculated to be roughly 70 and 30% according to the residual ratio, which was closely consistent with the initial feed ratio of cellulose and AC (2/1, m/m). These data strongly reveal that AC was successfully doped into the cellulose monolith.

Adsorption of a single dye by cellulose/AC composite monolith

The dye adsorption on the cellulose monolith and the cellulose/AC composite monolith was carried out at different contact times (Fig. 4). In this study, two types of dyes, MB and RhB, were used; the former is a cationic dye and the latter is a betaine one. The adsorption of MB and RhB dyes took place quickly for both adsorbents in the initial phase and gradually attained equilibrium. This is because the macroporous channel of the two adsorbents provides abundant space for the rapid transfer of large molecules. Interestingly, both dyes were adsorbed on the cellulose monolith, which may be because the cellulose monolith had mesopores (Fig. 3b). The cellulose monolith had equilibrium capacities of 5.70 mg g^{-1} (for MB) and 8.97 mg g^{-1} (for RhB) at the initial dye concentration of 200 mg L^{-1}, respectively. For both dyes, the equilibrium adsorption capacity of the composite monolith was obviously larger than that of the cellulose monolith. The higher equilibrium adsorption capacities of 26.7 and 13.0 mg g^{-1} were observed for the adsorption of MB and RhB on the cellulose/AC composite monolith under the same initial concentration, respectively. This difference is related to the predominant mesoporous structure and large specific surface area of the cellulose/AC monolith, resulting in an increase of mass permeability. Therefore, it can be concluded that the cellulose/AC monolith is a promising adsorbent in separation and adsorption applications.

Fig. 4 MB adsorption (**a**) and RhB adsorption (**b**) on the cellulose monolith and the cellulose/AC composite monolith at different times (C_0: 200 mg L^{-1}, pH 7 (MB), pH 3 (RhB), temperature: 298 K, adsorbent dosage: 0.10 g)
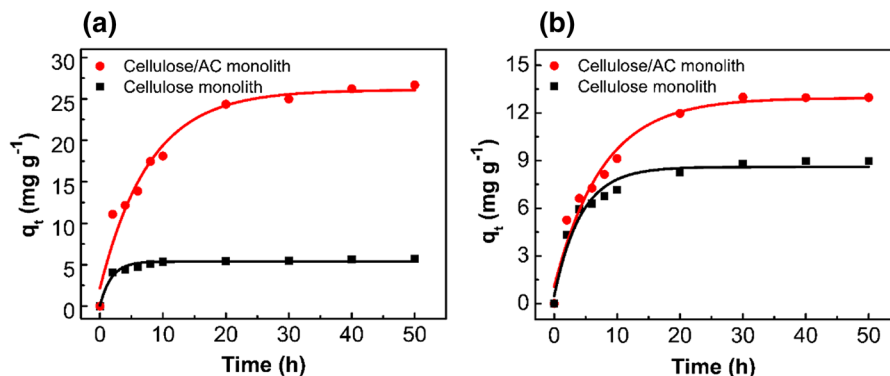
Influence factors of the adsorption process

Effects of pH

Figure 5 indicates the relationship between the pH of the initial solution and the adsorption capacity of the composite monolith toward both dyes at a constant contact time (50 h). The pH of the dye solution greatly influenced the adsorption capacity of the composite monolith. For MB, the adsorption capacity increased as a function of pH from 2 to 7, while beyond pH 7, the capacity was almost constant. The highest uptake of 26.2 mg g^{-1} was obtained at pH 8. This is due to the electrostatic repulsion of MB under the acidic conditions in which the positive charge on the surface of adsorbent was unfavorable for adsorption of the cationic dye. With the increase of pH, the available charge density for the adsorption increased and the capacity of MB adsorption markedly increased. In the treatment of dye wastewater, the solution is generally
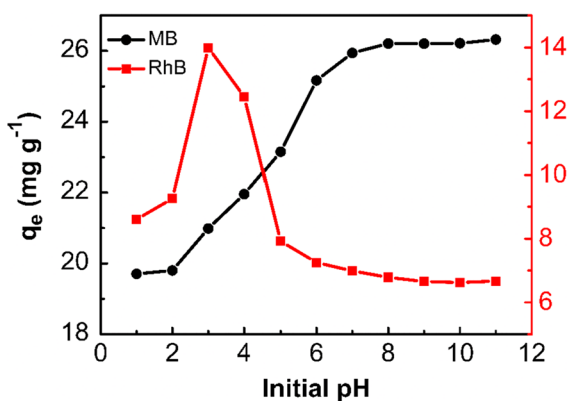
required to be neutral. Therefore, pH 7 was chosen as the ideal value of the initial MB solution.

In the case of RhB, the adsorption capacity increased with the increase of pH and reached the maximum value at pH 3. The adsorption capacity sharply declined with a further increase of pH until pH 9, when it reached a steady phase. RhB may exist as three different forms depending on the solution pH, cationic (RhBH$_2^{2+}$, pH < 1), lactonic (RhBH$^+$, pH 1–3), and zwitterionic. RhB is mainly in the form of zwitterionic at a pH higher than 3. The zwitterionic form strengthens the mutual attraction between the xanthene and the carboxyl groups of RhB molecules, resulting in the formation of the RhB dimer. It is very difficult for the dimer form to enter into the pores, causing adsorption of RhB onto the cellulose/AC composite monolith to subsequently decrease (Shakir et al. 2010). Furthermore, the decrease of RhB adsorption at pH lower than 3 is related to the competition from the protons of the positive dye cations.

Effects of initial dyes' concentrations and contact time

The effects of initial concentration and contact time on the adsorption onto the composite monolith were examined at pH 7 for MB and pH 3 for RhB at 298 K (Fig. 6). A similar varying tendency was observed for both the MB and RhB dyes. The adsorption rate increased with the increase of both contact time and concentration. The adsorption presented a rapid trend in the initial 10 h for all the concentrations of both dyes, because there were abundant active sites for the composite monolith to accelerate MB and RhB adsorption (Chairat et al. 2005) at the initial stage. Afterward, the adsorption became slow and gradually achieved equilibrium in the course of time, as the

Fig. 5 pH effect on the adsorption capacity of the cellulose/AC composite monolith toward MB and RhB (C_0: 200 mg L^{-1}, temperature: 298 K, adsorbent dosage: 0.10 g)
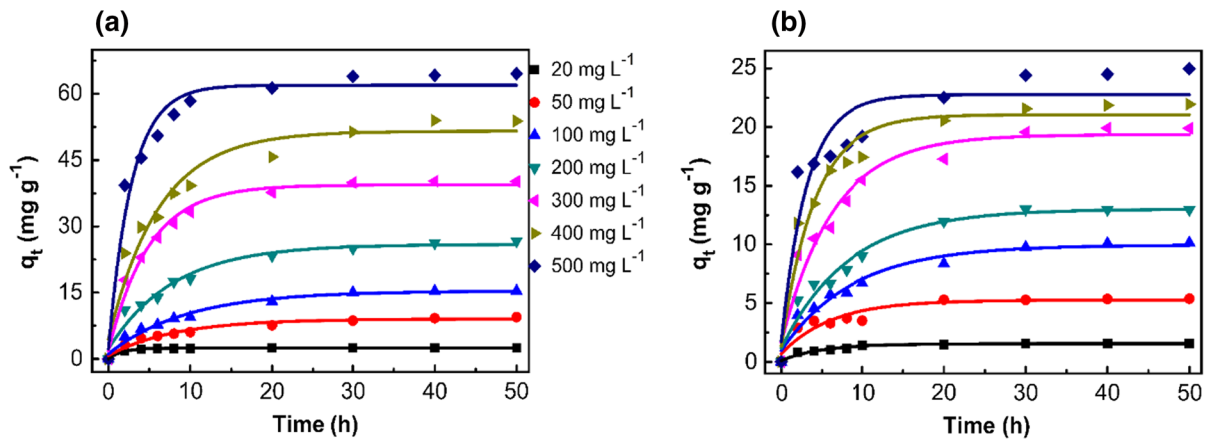
Fig. 6 Effect of contact time and initial concentrations toward MB adsorption (**a**) and RhB adsorption (**b**) onto the cellulose/AC composite monolith [pH 7 (MB), pH 3 (RhB), temperature: 298 K, adsorbent dosage: 0.10 g]

surface was now covered partially/completely by adsorbed dye molecules. In this phase, the pore diffusion of the adsorbed dye was very slow from the bulk phase to the particle surface (Malekbala et al. 2015). The equilibration time for the adsorption of MB was 30 h for the initial concentration of 10, 50, 100, and 200 mg L^{-1}, and at 50 h for the initial concentrations of 400 and 500 mg L^{-1}. On the other hand, the equilibrium for RhB was reached at 50 h except for the initial concentrations of 10 and 50 mg L^{-1}. The adsorption capacities were enhanced with increasing the initial dye concentration, which is probably because the higher dye concentration could offer a stronger driving force to overcome the mass transfer resistance between the solid phases (Ai et al. 2014). The equilibrium adsorption capacity of MB ranged from 2.5 to 65 mg g^{-1} as the initial concentration increased from 20 to 500 mg L^{-1}. The adsorption capacities of RhB were 1.6–25.0 mg g^{-1} at the concentration ranging from 10 to 500 mg L^{-1}. These data demonstrate that the high initial concentration does favor dye adsorption and sufficient use of the adsorbent. Thus, at higher practical wastewater concentrations, better adsorption efficiency and more sufficient utilization of the adsorbent can be obtained due to more active sites and adsorption surface (Yang et al. 2013; Zhang et al. 2016).

Effects of adsorbent dosage

The adsorbent dosage was dependent upon the adsorption capacity and removal efficiency (Fig. 7).

The influence was measured by the change of the dosage from 0.05 to 0.40 g. The removal efficiency for both dyes gradually increased with the increase of adsorbent dosage and finally attained equilibrium. As the adsorbent dosage increased, the surface area of the adsorbent became larger and more available adsorption sites were produced on the surface of cellulose/AC composite monolith. Hence, more dye molecules would be adsorbed, leading to a remarkable decrease of the residual concentration (Chen et al. 2011). At the adsorbent dosage of 0.30 g, a removal efficiency of 100% was observed for MB, whereas only 62% of RhB was adsorbed onto the composite monolith. Further addition of the composite monolith had little conspicuous influence toward dye removal. On the other hand, the adsorption capacities decreased with
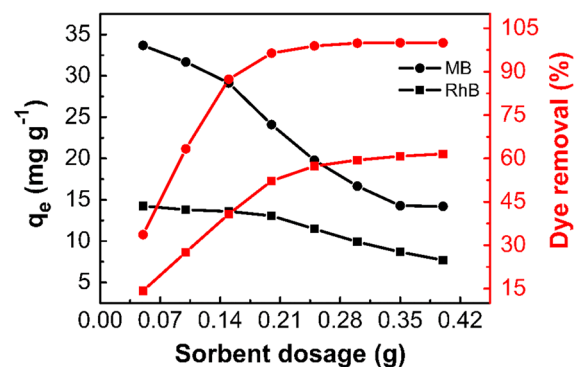
Fig. 7 Effect of cellulose/AC sorbent dosage on MB and RB adsorption capacity and MB and RhB removal efficiency (C_0: 200 mg L^{-1}, pH 7 (MB), pH 3 (RhB), temperature: 298 K)

the increase of adsorbent dosage for both dyes, which means that the adsorption capacities of both dyes did not reach saturation at the dye concentration of 200 mg L^{-1}. This can be explained by the abundant unsaturated sites reducing the adsorption density of the composite monolith, resulting in the decrease of the dye adsorbed per unit mass of adsorbent with increasing the adsorbent mass.

Effects of temperature

Figure 8 shows the effects of temperature on the adsorption of both dyes onto the composite monolith. The evaluation was carried out under the condition of pH 7 for MB and pH 3 for RhB, with an adsorbent increasing temperature, and the adsorption capacity for MB increased from 26.7 to 50.0 mg g^{-1} when the temperature increased from 298 to 333 K, indicating that the adsorption process was endothermic in nature. Similarly, the variation trend was found for RhB. The amounts of RhB adsorbed were 13.0, 35.6,and 43.0 mg g^{-1} at temperatures of 298, 313 and 333 K, respectively. These data could be explained as follows. At higher temperature, the movability of the dye molecules accelerated and promoted more molecules to be in contact with active sites of the adsorbent surface, leading to the larger adsorption capacity (Malekbala et al. 2015).

Simultaneous adsorption of two dyes

To further test the adsorption capacity of the cellulose/AC composite monolith, a solution containing a mixture of MB and RhB in a 1:1 weight ratio was subjected to adsorption at pH 7. UV/vis spectra (Fig. 9a) clearly showed that the absorption peaks of

MB and RhB simultaneously became smaller in the course of time. These data indicate that both MB and RhB were removed by the composite monolith, corresponding to the digital images as shown in Fig. 9b; the solution color changed from deep blue to light purple. The adsorption rate for the mixed dye solution was lower than that of the sole dye (MB or RhB).

Interestingly, the adsorption capacity of both dyes from the mixture system much improved in comparison with that of the sole dye solution (Fig. S4). Especially,an enormous improvement of the adsorption capacity was observed for RhB; 33.4 mg g^{-1} was obtained from the mixture after 50 h, which was larger than that of the single dye of RhB (13.0 mg g^{-1}). For this system, the total concentration of the mixture was 400 mg L^{-1}, which was higher than the individual dye solution (200 mg L^{-1}). The increase of solution concentration played the key role of a driving force to overcome mass transfer resistance, making possible increasing collisions between the dye molecules and the surface of the composite monolith, thus resulting in higher adsorption capacity These data showed that the monolith had little serious competition and selective adsorption between MB and RhB, and that the efficient adsorption of both dyes on the composite monolith took place simultaneously.

Kinetic parameters

In order to elucidate the mechanism of the dye adsorption on the present composite monolith and design the control of the adsorption rate useful for practical applications, the kinetic parameters were determined through kinetics models. The kinetics was studied at different dye concentrations and temperatures. The fitting for pseudo-first-order and pseudo-

Fig. 8 Temperature effect on MB adsorption (a) and RhB adsorption (b) onto the cellulose/AC composite monolith [C_0: 200 mg L^{-1}, pH 7 (MB), pH 3 (RhB), adsorbent dosage: 0.10 g]
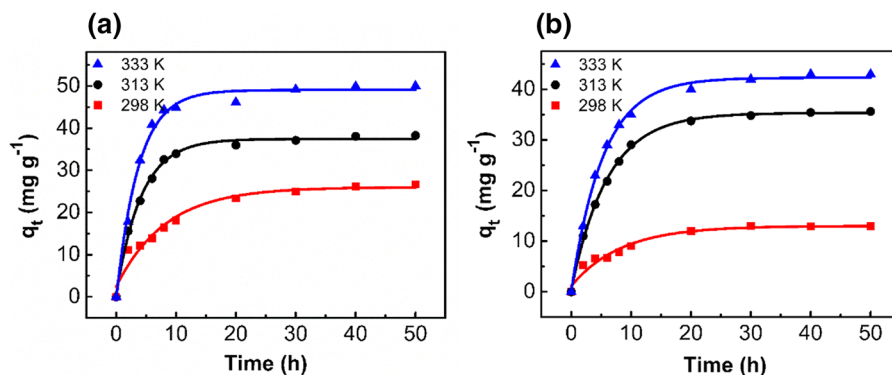
Fig. 9 Adsorption capability of the cellulose/AC composite monolith toward the mixed dye of MB and RhB (a), digital image of the mixed dye solution after adsorption experiments at given intervals (b) (C_0: 200 mg L^{-1}, pH 7, temperature: 298 K, adsorbent dosage: 0.10 g)
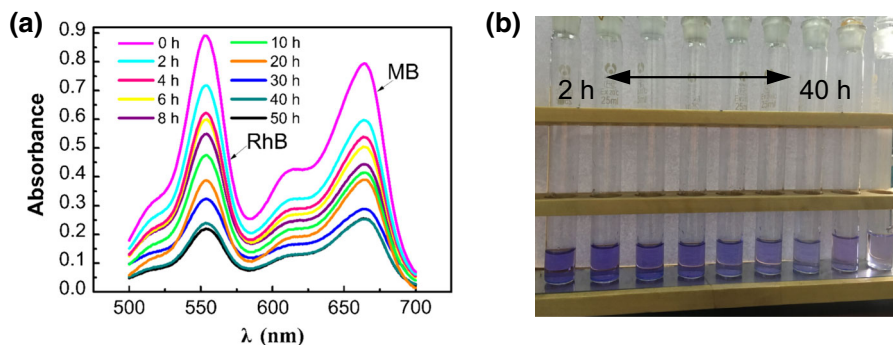
Table 2 Correlated parameters of the kinetic data for the adsorption of RhB onto cellulose/AC composite monolith with the temperature at 298, 303 and 333 K according to the pseudo-first-order and pseudo-second-order rate equations [C_0: 200 mg, pH 3 (RhB), adsorbent dosage: 0.10 g]

T (K)	Pseudo-first-order			$q_{e,exp}$ (mg g^{-1})	Pseudo-second-order		
	k_1 (h^{-1})	$q_{e,cal}$ (mg g^{-1})	R^2		k_2 (g mg^{-1} min^{-1})	$q_{e,cal}$ (mg g^{-1})	R^2
298	0.181	18.4	0.966	13.0	1.23×10^{-2}	14.9	0.994
303	0.0997	24.2	0.971	35.6	4.89×10^{-3}	40.5	0.998
333	0.0856	26.2	0.969	43.0	5.41×10^{-3}	47.4	0.999

second-order models in the adsorption of MB and RhB with different initial concentrations and temperatures has been examined (Figs. S5–S7). Figure S5a, b shows the fitting linear graphs of the pseudo-second-order model for MB and RhB under different initial concentrations, respectively. All the kinetic parameters are summarized in Tables S1 and S2. Figures S6 and S7 demonstrate fitting plots of two kinetic models toward MB and RhB at different temperatures, respectively. All the kinetic parameters are given in Tables S3 and 2. A remarkable linearity of the plots (correlation coefficients $R^2 > 0.99$) and good agreement between the calculated value of adsorption capacity ($q_{e, cal}$) and the experimental one ($q_{e, exp}$) were observed, which indicates that the adsorption of MB and RhB onto the composite monolith can be well-fitted to the pseudo-second-order model. Moreover, the equilibrium adsorption capacity increased with the increase of the initial MB concentration, which would be caused by the relatively strong driving force under high dye concentrations.

Isotherm studies

The adsorption isotherm is used to describe the distribution of dye molecules on the surface of the solid phase adsorbent when the adsorption process reaches an equilibrium state. The adsorption isotherms of MB and RhB are shown in Fig. 10, and the corresponding fitted results are listed in Table 3. The correlation coefficient, R^2, of the Freundlich model was larger than that of the Langmuir model for RhB adsorption. A higher correlation coefficient of the Freundlich model ($R^2 > 0.98$) was also observed for MB. Thus, the present adsorption was proved to obey the Freundlich model by the equilibrium data. This result suggests that the surface of the cellulose/AC composite monolith is heterogeneous, with a rough and porous morphology with a hierarchical porous structure, resulting in the multilayer adsorption. Additionally, the n values are higher than 1 for both dyes, implying that the adsorption process was favorable. From these data, the composite monolith will possess a high potential for practical treatment of dye wastewater.

Desorption and recyclability

The good stability and reusability of target materials are another important standard for inexpensive practical applications; thus, a study of the regeneration of
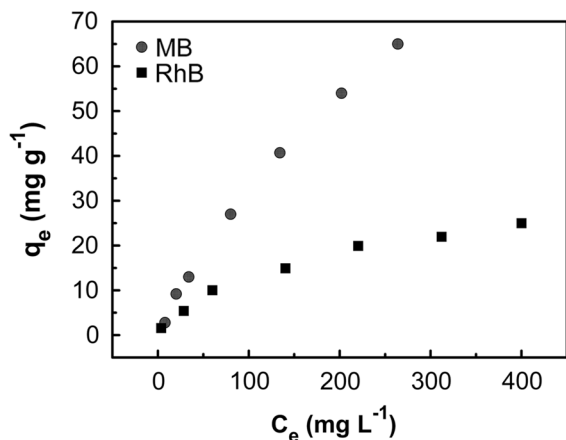
Fig. 10 Adsorption isotherms of MB and RB onto cellulose/AC composite monolith [pH 7 (MB), pH 3 (RhB), temperature: 298 K, adsorbent dosage: 0.10 g]

Fig. 11 Regeneration and repeated use of the cellulose/AC composite using 99% of ethanol for 8 cycles (C_0: 400 mg L^{-1}, pH 7 (MB), pH 3 (RhB), temperature: 298 K, adsorbent dosage: 0.10 g)

the adsorbent is strongly required. Desorption experiments were performed by the use of 99% ethanol as desorption agent for the regeneration of the cellulose/AC composite, and this release process was also examined by different concentrations of HCl treatment. Fast and efficient desorption of dyes was observed in 99% ethanol. When 99% ethanol was used as desorption agent, the desorption process could reach equilibrium within 3 h, and 94.0 and 98.0% of desorption ratio were obtained for MB and RhB, respectively.

The recyclability of the cellulose/AC monolith was investigated by repeating the adsorption–desorption process 8 times. The adsorption capacity hardly changed for either of the dyes for the first three times. The adsorption ratio still retained 89% for MB and 93% for RhB after 8 successive cycles (MB dropped from 53.4 to 46.2 mg g^{-1}, and RhB decreased from 26.3 to 23.6 mg g^{-1}) in comparison with the original adsorption capacity (Fig. 11). These data clearly indicate that the current material has a remarkably efficient regeneration capability.

Conclusion

In summary, a hierarchical mesoporous cellulose/AC composite monolith was successfully synthesized through TIPS with a simple and facile method, which could be used as an efficient and recyclable monolithic adsorbent for applications of dye wastewater treatment. The as-obtained composite monolith exhibited high performance for the removal of a single dye (MB or RhB) from an aqueous solution, with the maximum adsorption capacities for MB and RhB being 159 and 33.4 mg g^{-1} (Table 3), respectively. The kinetics and isotherm studies showed that the adsorption obeyed pseudo-second-order kinetics and the Freundlich isotherm model, respectively. Interestingly, the present composite monolith also showed the higher uptake capacity toward a mixture of MB and RhB. Furthermore, the composite monolith was also stable in reuse; it still kept an excellent adsorption capacity towards MB and RhB after 8 successive adsorption–desorption cycles. The current materials with easy morphology control, easy solid–liquid

Table 3 Isotherm parameters for MB and RB adsorption onto the cellulose/AC composite monolith [pH 7 (MB), pH 3 (RhB), temperature: 298 K, adsorbent dosage: 0.10 g]

	Langmuir constants			Freundlich constants		
	K_L (L mg^{-1})	q_m (mg g^{-1})	R^2	K_F (mg g^{-1}) (L mg^{-1})$^{1/n}$	n	R^2
MB	2.60×10^{-3}	158	0.892	0.573	1.16	0.986
RhB	6.64×10^{-3}	33.4	0.990	0.744	1.66	0.992

separation, and fast mass transfer could be used as promising practical candidates for environmental improvement.

Author contributions The paper was written through contributions of all authors. All authors have given approval to the final version of the paper.

Compliance with ethical standards

Conflicts of interest The authors declare no conflict of interest related to this research work.

References

Ai L, Zeng Y, Jiang J (2014) Hierarchical porous BiOI architectures: facile microwave nonaqueous synthesis, characterization and application in the removal of Congo red from aqueous solution. Chem Eng J 235:331–339

Balathanigaimani M, Lee M-J, Shim W-G, Lee J-W, Moon H (2008) Charge and discharge of methane on phenol-based carbon monolith. Adsorption 14:525–532

Balathanigaimani MS, Shim W-G, Lee J-W, Moon H (2009) Adsorption of methane on novel corn grain-based carbon monoliths. Microporous Mesoporous Mater 119:47–52

Bradbury AGW, Sakai Y, Shafizadeh F (1979) A kinetic model for pyrolysis of cellulose. J Appl Polym Sci 23:3271–3280

Chairat M, Rattanaphani S, Bremner JB, Rattanaphani V (2005) An adsorption and kinetic study of lac dyeing on silk. Dyes Pigments 64:231–241

Chen S, Yue Q, Gao B, Li Q, Xu X (2011) Removal of Cr(VI) from aqueous solution using modified corn stalks: characteristic, equilibrium, kinetic and thermodynamic study. Chem Eng J 168:909–917

Choong TS, Wong TN, Chuah TG, Idris A (2006) Film-pore-concentration-dependent surface diffusion model for the adsorption of dye onto palm kernel shell activated carbon. J Colloid Interface Sci 301:436–440

Coleman N, Hench L (2000) A gel-derived mesoporous silica reference material for surface analysis by gas sorption 1. Textural features. Ceram Int 26:171–178

Dong Z, Wang D, Liu X, Pei X, Chen L, Jin J (2014) Bio-inspired surface-functionalization of graphene oxide for the adsorption of organic dyes and heavy metal ions with a superhigh capacity. J Mater Chem A 2:5034–5040

Dridi-Dhaouadi S, Douissa-Lazreg NB, M'Henni MF (2011) Removal of lead and Yellow 44 acid dye in single and binary component systems by raw *Posidonia oceanica* and

the cellulose extracted from the raw biomass. Environ Technol 32:325–340

Freundlich HMF (1906) Over the adsorption in solution. J Phys Chem A 57:385–470

Gopiraman M, Bang H, Yuan G, Yin C, Song KH, Lee JS et al (2015) Noble metal/functionalized cellulose nanofiber composites for catalytic applications. Carbohydr Polym 132:554–564

He X, Male KB, Nesterenko PN, Brabazon D, Paull B, Luong JH (2013) Adsorption and desorption of methylene blue on porous carbon monoliths and nanocrystalline cellulose. ACS Appl Mater Interfaces 5:8796–8804

Ho Y-S, McKay G (1999) Pseudo-second order model for sorption processes. Process Biochem 34:451–465

Kyzas GZ, Bikiaris DN (2015) Recent modifications of chitosan for adsorption applications: a critical and systematic review. Mar Drugs 13:312–337

Lagergren S (1898) Zur Theorie der Sogenannten Adsorption Geloester Stoffe. Kungliga Sven Vetensk Handl 24:1–39

Langmuir I (1916) The constitution and fundamental properties of solids and liquids. Part I. Solids J Am Chem Soc 38:2221–2295

Lillo-Ródenas MA, Cazorla-Amorós D, Linares-Solano A (2010) Benzene and toluene adsorption at low concentration on activated carbon fibres. Adsorption 17:473–481

Liu K, Chen L, Huang L, Lai Y (2016) Evaluation of ethylene-diamine-modified nanofibrillated cellulose/chitosan composites on adsorption of cationic and anionic dyes from aqueous solution. Carbohydr Polym 151:1115–1119

Malekbala MR, Khan MA, Hosseini S, Abdullah LC, Choong TSY (2015) Adsorption/desorption of cationic dye on surfactant modified mesoporous carbon coated monolith: equilibrium, kinetic and thermodynamic studies. J Ind Eng Chem 21:369–377

Menon V, Komarneni S (1998) Porous adsorbents for vehicular natural gas storage: a review. J Porous Mater 5:43–58

Okada K, Nandi M, Maruyama J, Oka T, Tsujimoto T, Kondoh K, Uyama H (2011) Fabrication of mesoporous polymer monolith: a template-free approach. Chem Commun 47:7422–7424

Park SB, Fujimoto T, Mizohata E, Inoue T, Sung MH, Uyama H (2013) Fabrication of poly (gamma-glutamic acid) monolith by thermally induced phase separation and its application. J Microbiol Biotechnol 23:942–952

Radha G, Balakumar S, Venkatesan B, Vellaichamy E (2017) A novel nano-hydroxyapatite—PMMA hybrid scaffolds adopted by conjugated thermal induced phase separation (TIPS) and wet-chemical approach: analysis of its mechanical and biological properties. Mater Sci Eng C 73:164–172

Shakir K, Elkafrawy AF, Ghoneimy HF, Elrab Beheir SG, Refaat M (2010) Removal of rhodamine B (a basic dye) and thoron (an acidic dye) from dilute aqueous solutions and wastewater simulants by ion flotation. Water Res 44:1449–1461

Sun X, Uyama H (2013) A poly (vinyl alcohol)/sodium alginate blend monolith with nanoscale porous structure. Nanoscale Res Lett 8:4745–4751

Sun X, Fujimoto T, Uyama H (2013) Fabrication of a poly (vinyl alcohol) monolith via thermally impacted non-solvent-induced phase separation. Polym J 45:1101–1106

Wang G, Uyama H (2015) Reactive poly (ethylene-*co*-vinyl alcohol) monoliths with tunable pore morphology for enzyme immobilization. Colloid Polym Sci 293: 2429–2435

Wang G, Xin Y, Uyama H (2015) Facile fabrication of mesoporous poly (ethylene-co-vinyl alcohol)/chitosan blend monoliths. Carbohydr Polym 132:345–350

Wu Z, Cheng Z, Ma W (2012) Adsorption of Pb(II) from glucose solution on thiol-functionalized cellulosic biomass. Bioresour Technol 104:807–809

Xin Y, Fujimoto T, Uyama H (2012) Facile fabrication of polycarbonate monolith by non-solvent induced phase separation method. Polymer 53:2847–2853

Xin Y, Xiong Q, Bai Q, Miyamoto M, Li C, Shen Y, Uyama H (2017) A hierarchically porous cellulose monolith: a template-free fabricated, morphology-tunable, and easily functionalizable platform. Carbohydr Polym 157:429–437

Yang S, Zhao Y, Chen R, Feng C, Zhang Z, Lei Z, Yang Y (2013) A novel tablet porous material developed as adsorbent for phosphate removal and recycling. J Colloid Interface Sci 396:197–204

Yi FY, Zhu W, Dang S, Li JP, Wu D, Li YH, Sun ZM (2015) Polyoxometalates-based heterometallic organic–inorganic hybrid materials for rapid adsorption and selective separation of methylene blue from aqueous solutions. Chem Commun 51:3336–3339

Yoneda S, Han W, Hasegawa U, Uyama H (2014) Facile fabrication of poly (methyl methacrylate) monolith via thermally induced phase separation by utilizing unique cosolvency. Polymer 55:3212–3216

Zhang L, Gao H, Liao Y (2016) Preparation and application of Poly(AMPS-co-DVB) to remove Rhodamine B from aqueous solutions. React Funct Polym 104:53–61

Zhu HY, Fu YQ, Jiang R, Jiang JH, Xiao L, Zeng GM et al (2011) Adsorption removal of congo red onto magnetic cellulose/Fe_3O_4/activated carbon composite: equilibrium, kinetic and thermodynamic studies. Chem Eng J 173: 494–502